Harmonic modeling of vibration energy harvesting systems using extended impedance method

IOP Conf. Series: Materials Science and Engineering **531** (2019) 012083 doi:10.1088/1757-899X/531/1/012083

Harmonic modeling of vibration energy harvesting systems using extended impedance method

Yiming Gao[1], Bao Zhao[1], Jiahua Wang[2], and Junrui Liang[1]

[1] School of Information Science and Technology, ShanghaiTech University, Shanghai 201210, China

[2] Department of Mechanical and Automation Engineering, The Chinese University of Hong Kong, Hong Kong, China

E-mail: liangjr@shanghaitech.edu.cn

Abstract. Vibration energy harvesting (VEH) systems convert the mechanical vibration energy in AC form into storable electrical energy in DC form. The mechanical structure, electromechanical transducer, and power electronics are three necessary parts for realizing the electromechanical energy transduction and rectification. The difficulty was found in modeling the electromechanical joint dynamics, in particular, when complex mechanical dynamics or sophisticated electrical switching transient are involved. Harmonic analysis is proven to be an efficient tool for modeling such a multiple-field-coupled power conversion system. In this paper, we develop a multiple harmonics analysis for the piezoelectric energy harvesting systems based on the extended impedance method (EIM). This method was used in the analysis of nonlinear power electronic circuits, such as resonant inverters and dc-dc converters. The theoretical results at steady state are compared with the simulation results from the commercialized circuit simulation software. The new modeling technique provides an efficient tool for the customized design and holistic optimization of the vibration energy harvesting systems.

1. Introduction

Piezoelectric energy harvesting (PEH) is a kind of VEH technology which provides promising opportunities towards the self-powered IoT (Internet of Things) devices. With the emerging power conditioning circuits, the output power and power bandwidth of the PEH system have been improved a lot during the last decade. By using the synchronized switch solutions, which manipulate the piezoelectric voltage at its extreme points, the energy harvesting capability can be enhanced by several folds. The first synchronized switch harvesting on inductor (SSHI) [1] solution was proposed in 2005. Liang et al. have proposed the parallel synchronized triple bias-flip (P-S3BF) [2] by introducing three switching actions. Gasnier et al. have expanded the synchronized switch concept and realized the multi-shot synchronous electric charge extraction (MS-SECE) into IC application [3].

Besides the circuit improvement, how to simulate the holistic electromechanical system, analyze the interaction between the mechanical side and electrical side has been an important issue for the study of PEH systems. Conventional analyses can be mainly divided into two categories. Early methods model the PEH system as an ideal source under constant displacement excitation [1, 4] or constant force excitation [5]. Given the insufficiency of the uncoupled models, Shu et al. [6] have proposed the energy balance analysis for PEH systems using P-SSHI and

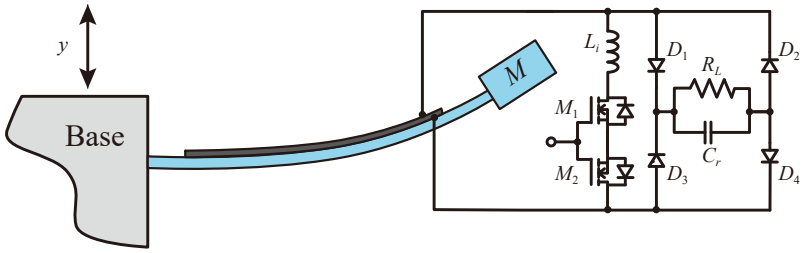

Figure 1. A PEH system using P-SSHI interface circuit.

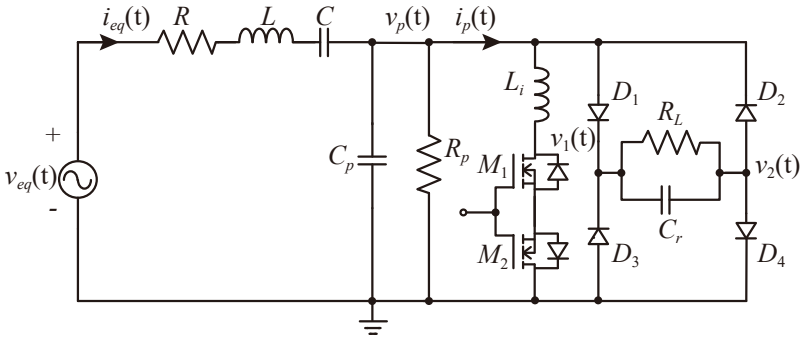

Figure 2. Equivalent circuit model.

S-SSHI interface circuits. On the other hand, with different underlying concepts, Liang et al. [7] have analyzed the joint dynamics base on the fundamental harmonic impedance analysis. The similar harmonic based concept was used in PEH systems with complex mechanical dynamics [8, 9].

In PEH analysis, what we mostly care about is the steady-state performance. But through time-domain simulation, the transient analysis is inevitable and consume extra computational afford. Different from the aforementioned methods, the extended impedance method (EIM) uses the harmonic concept to form nonlinear conductance or impedance in the frequency domain. By using EIM, the whole circuit can be solved in the frequency domain. Steady-state waveforms can be obtained immediately even nonlinear components and nonlinear control exist.

In the previous studies, EIM was used to analyze the nonlinear circuit such as the Class-E amplifier. [10, 11, 12, 13]. It outperforms other simulation methods in both computational efficiency and intuitive understanding. In this paper, the EIM is migrated to analyze the SSHI interface circuit in PEH system, which has utilized some nonlinear components and nonlinear control method. The EIM provides another efficient way for the analysis and optimization of the practical SSHI interface circuit.

2. EIM Modeling

As illustrated in Fig. 1, a PEH system with SSHI interface circuit consists of the mechanical structure and electrical interface circuit. Its mechanical part is a cantilever beam, which acts as the energy source. The SSHI interface is introduced. In SSHI, the nonlinear control and switch-mode nonlinear components are utilized to improve the power factor and enhance the harvested power. EIM is able to describe such nonlinearity using harmonic modeling.

2.1. Mechanical to electrical analogy

In this paper, the system is subjected to harmonic base excitation. The governing equations of the single-degree-freedom (SDOF) system can be described as follows

$$\begin{cases} M\ddot{x}(t) + D\dot{x}(t) + (K + K_p)x(t) + \alpha_e v_p(t) = -M\ddot{y}(t), \\ i_p(t) = \alpha_e \dot{x}(t) - C_p \dot{v_p}(t) - \frac{1}{R_p} v_p(t), \end{cases} \tag{1}$$

where M, D, K, and K_p represent the equivalent mass, mechanical damping (dissipation), substrate stiffness, and piezoelectric short circuit stiffness, respectively; C_p is the piezoelectric clamped capacitance; R_p is the dielectric resistance of the piezoelectric element; v_p is the voltage across the piezoelectric element, and i_p is the current flowing through the element; α_e is the force-voltage factor of the piezoelectric transducer. The base acceleration $\ddot{y}(t)$, the second derivative of the base displacement $y(t)$, is the mechanical excitation.

According to the electromechanical analogy [7, 14]

$$q(t) = \alpha_e x(t) \tag{2}$$

$$v_{eq}(t) = -\frac{M}{\alpha_e}\ddot{y}(t) \tag{3}$$

$$L = \frac{M}{\alpha_e^2} \tag{4}$$

$$R = \frac{D}{\alpha_e^2} \tag{5}$$

$$C = \frac{\alpha_e^2}{K + K_p} \tag{6}$$

the mechanical side displacement, base excitation, mass, damping, and stiffness can be analogized as the charge, voltage source, inductance, resistance, and capacitance in the electrical domain, respectively, as shown in Fig. 2

2.2. EIM model

The whole equivalent circuit model of PEH and P-SSHI interface circuit has shown in Fig. 2, which contains some linear components such as resistance, inductance, capacitance and some nonlinear components such as MOSFETs and diodes and even nonlinear control of the MOSFET gate signal.

From a broader point of view, the nonlinear components can also be regarded as special resistors as shown in Fig. 3. Their resistances are determined by the terminal voltage and gate control signal.

The four diodes D_1 to D_4 can be modeled as nonlinear resistance R_{di} $(i = 1, 2, 3, 4)$ which is described with the following equation

$$R_{di} = \begin{cases} \infty, & v_d \le 0; \\ \frac{v_d}{I_s[e^{-v_d/(nV_T)} - 1]}, & v_d > 0, \end{cases} \tag{7}$$

where v_d, I_s, n, V are the forward diode voltage, saturation current, thermal voltage, and ideal factor, respectively.

The two power MOSFETs M_1 and M_2, are modeled as a nonlinear resistance R_{sw}, whose value is determined by the phase of current i_{eq} according to the following relation

$$R_{sw}(t) = \begin{cases} R_{on}, & t_{zc} < t < t_{zc} + \pi\sqrt{L_i C_p}; \\ R_{off}, & \text{other}, \end{cases} \tag{8}$$

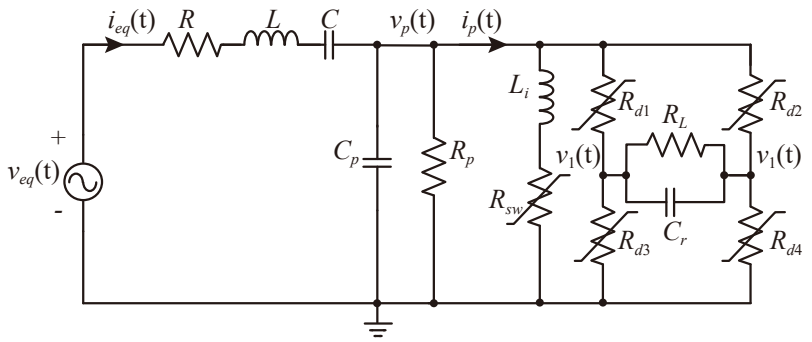

Figure 3. The EIM model.

where t_{zc} is the zero-crossing instants of i_{eq}, and $\pi\sqrt{L_iC_p}$ is half of an LC resonant cycle.

With such equivalent transformation, all the components in Fig. 3 can be regarded as impedance in frequency domain. In EIM, the impedance of each component is no longer expressed as conventional complex scalar, but complex matrices [11]. The PEH equivalent circuit can be easily formulated by using the nodal analysis. The circuit constitutive equation is expressed as follows.

$$\begin{bmatrix} \boldsymbol{V_p}^{(n+1)} \\ \boldsymbol{V_1}^{(n+1)} \\ \boldsymbol{V_2}^{(n+1)} \end{bmatrix} = \begin{bmatrix} \boldsymbol{Y_p}^{(n)} & -\boldsymbol{Y_{d1}}^{(n)} & -\boldsymbol{Y_{d2}}^{(n)} \\ -\boldsymbol{Y_{d1}}^{(n)} & \boldsymbol{Y_{d1}}^{(n)} + \boldsymbol{Y_{d3}}^{(n)} + \boldsymbol{Y_{load}} & -\boldsymbol{Y_{load}} \\ -\boldsymbol{Y_{d2}}^{(n)} & -\boldsymbol{Y_{load}} & \boldsymbol{Y_{load}} + \boldsymbol{Y_{d2}}^{(n)} + \boldsymbol{Y_{d4}}^{(n)} \end{bmatrix}^{-1} \begin{bmatrix} \boldsymbol{Y_{RLC}}\boldsymbol{V_{eq}}^{(n)} \\ \boldsymbol{0} \\ \boldsymbol{0} \end{bmatrix} \tag{9}$$

where

$$\boldsymbol{Y_p}^{(n)} = \boldsymbol{Y_{RLC}} + \boldsymbol{Y_{Cp}} + \boldsymbol{Y_{Rp}} + \boldsymbol{Y_{swLi}}^{(n)} + \boldsymbol{Y_{d1}}^{(n)} + \boldsymbol{Y_{d2}}^{(n)} \tag{10}$$

$$\boldsymbol{Y_{swLi}} = (\boldsymbol{Z_{sw}}^{(n)} + \boldsymbol{Z_{Li}})^{-1} \tag{11}$$

$$\boldsymbol{Y_{RLC}} = (\boldsymbol{Z_R} + \boldsymbol{Z_L} + \boldsymbol{Z_C})^{-1} \tag{12}$$

$$\boldsymbol{Y_{load}} = \boldsymbol{Y_{RL}} + \boldsymbol{Y_{Cr}} \tag{13}$$

The three nodes other than the ground are denoted as the vectors $\boldsymbol{V_p}$, $\boldsymbol{V_1}$, and $\boldsymbol{V_2}$. The vector $\boldsymbol{V_{eq}}$ is the equivalent excitation in the frequency domain. $\boldsymbol{Y_x}$ and $\boldsymbol{Z_x}$ are the admittance and impedance of the corresponding $\boldsymbol{x}$ component. The superscript (n) and (n+1) denote the number of iterations. The voltage vectors, whose length are $2K+1$, stand for the steady-state voltages in frequency domain with the harmonic order of K. The admittance matrices, whose dimensions are $(2K+1)^2$, express the characterizes of their corresponding component. The linear components give diagonal admittance matrices.

Starting with an initially estimated voltage vector, all the extended admittance matrices are able to be obtained. In the next iteration, the constitutive relation runs to acquire the new voltage results. Such a process continues until the relative error between two iteration results satisfies the tolerant requirement. Fig. 4 summarizes the simulation processes of the EIM based PEH and SSHI interface circuit analysis.

3. Model validation

The time-domain simulation using commercialized software are carried out to validate the proposed modeling using EIM. The system parameters listed in Table 1 are measured by impedance analyzer and indirectly obtained. With these parameters, a MATLAB program

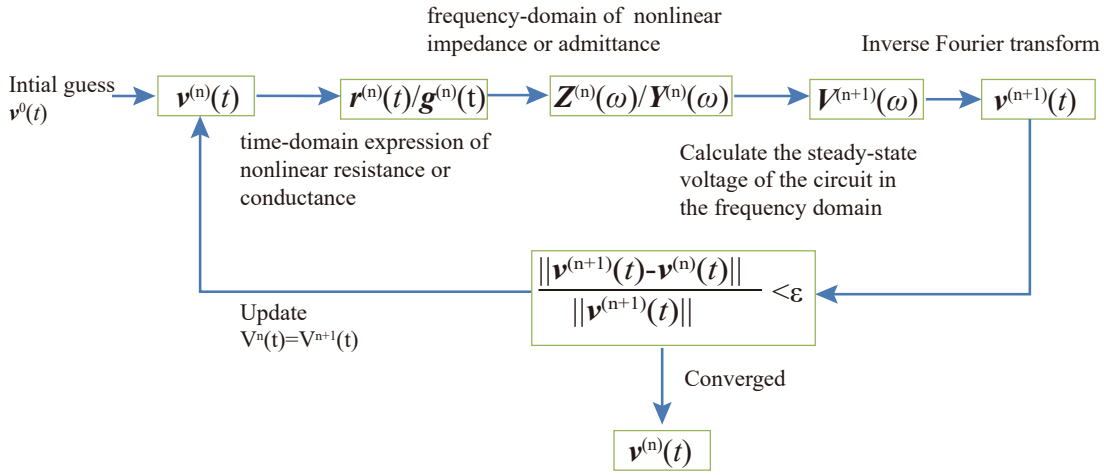

Figure 4. Flow Chart for the EIM based PEH interface circuit analysis.

Table 1. Parameters of PEH system using SSHI interface circuit.

Parameter	Value	Parameter	Value
R	345.47 kΩ	L_i	47 mH
L	31.18 kH	C_r	10 μF
C	0.27 nF	ω	$2\pi \times 54.8$ rad/s
C_p	45.7 nF	α_e	0.37×10^{-3} N/V
R_p	533.47 kΩ	k_e^2	5.9×10^{-3}
V_{eq}	100 V	γ	-0.85

based on EIM runs to acquire the steady-state voltages of the circuit. The harmonic order $K = 200$. From Fig. 5(a) the EIM simulation result, we can observe that when the piezoelectric structure is at open-circuit condition, i.e., $R_L = \infty$, the rectified voltage v_o is charged up to the maximum value of piezoelectric voltage v_p. When of v_p reaches the extreme values, at the same instant, piezoelectric equivalent current crosses zero, the MOSFETs turn on, enabling L_i and C_p form an under-damped resonant branch. Because the electrical resonant frequency is much higher than that of mechanical vibration. Thus v_p sharply jumps at the synchronized instants. The switch turns off after one half of the L_iC_p resonant cycle. After that v_p recharges in the reverse direction.

If the load resistance is 1 MΩ, the diodes can be conducted for some intervals in every cycle. From the simulation result in Fig. 5(b), it is observed that v_p has been clamped at a rectified voltage v_o. Compared with the simulation results obtained in PSIM software, the waveforms make a very good agreement, as Fig. 5(b) and Fig. 6(b) show. However, the difference is observed when load resistance R_L is infinite. From Fig. 6(a) the waveform of v_p in the PSIM simulation result, voltage clamping phenomenon still exists. The simulation does not accord with the theory. It is because the diode model in PSIM is not accurate enough to simulate the more precise dynamics circuit. On the contrary, EIM performs well for dealing with both nonlinear components and nonlinear control.

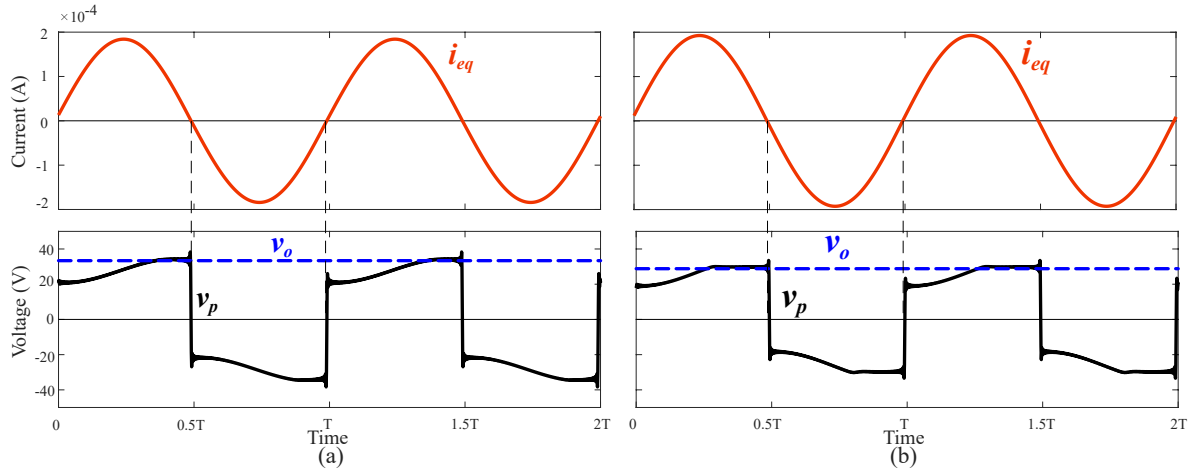

Figure 5. Steady-state waveforms obtained with EIM. (a) Open circuit ($R_L = \infty$). (b) $R_L = 1$ MΩ

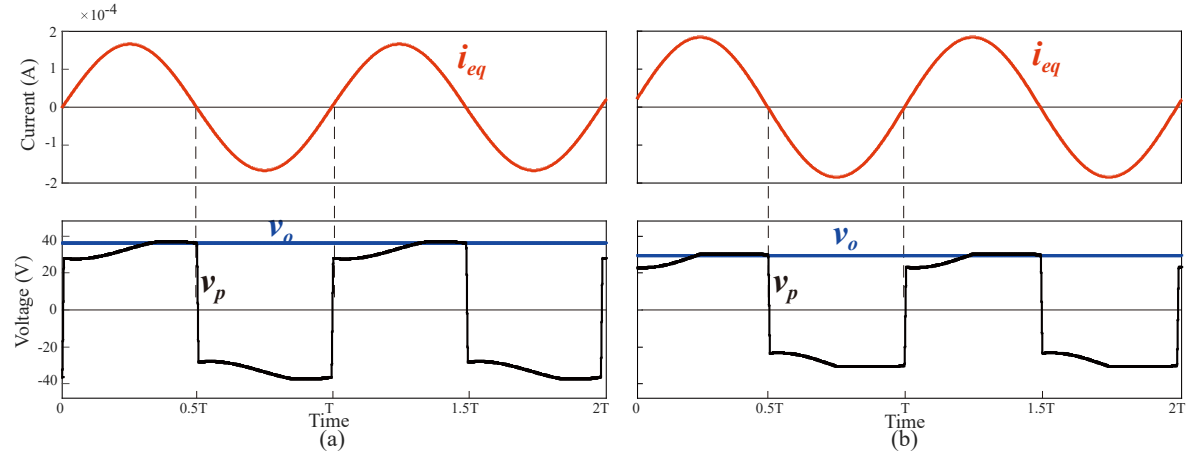

Figure 6. Steady-state waveforms obtained with PSIM. (a) Open circuit ($R_L = \infty$). (b) $R_L = 1$ MΩ

4. Conclusion

PEH technology is one of the most extensively investigated energy harvesting solutions. While the electromechanical joint dynamic of a PEH system is not easy to model. This paper combined the electromechanical analogy and EIM together, such that to use the extended impedance concept to deal with the nonlinear components and nonlinear control. The simulation result has demonstrated its advantage as it can simulate the dynamics more efficiently. In addition, thanks to its numerical feature, it has the potential to be applied to the model and optimize more complex nonlinear circuits.

References

[1] Daniel Guyomar, Adrien Badel, Elie Lefeuvre, and Claude Richard. Toward energy harvesting using active materials and conversion improvement by nonlinear processing. *IEEE transactions on ultrasonics, ferroelectrics, and frequency control*, 52(4):584–595, 2005.

[2] Junrui Liang, Yuheng Zhao, and Kang Zhao. Synchronized triple bias-flip interface circuit for piezoelectric energy harvesting enhancement. *IEEE Transactions on Power Electronics*, 34(1):275–286, 2019.

[3] Pierre Gasnier, Jerome Willemin, Sebastien Boisseau, Ghislain Despesse, Cyril Condemine, Guillaume

Gouvernet, and Jean-Jacques Chaillout. An autonomous piezoelectric energy harvesting ic based on a synchronous multi-shot technique. *IEEE Journal of Solid-State Circuits*, 49(7):1561–1570, 2014.

[4] WQ Liu, ZH Feng, J He, and RB Liu. Maximum mechanical energy harvesting strategy for a piezoelement. *Smart Materials and Structures*, 16(6):2130, 2007.

[5] Elie Lefeuvre, Adrien Badel, Claude Richard, Lionel Petit, and Daniel Guyomar. A comparison between several vibration-powered piezoelectric generators for standalone systems. *Sensors and Actuators A: Physical*, 126(2):405–416, 2006.

[6] YC Shu, IC Lien, and WJ Wu. An improved analysis of the sshi interface in piezoelectric energy harvesting. *Smart Materials and Structures*, 16(6):2253, 2007.

[7] Junrui Liang and Wei-Hsin Liao. Impedance modeling and analysis for piezoelectric energy harvesting systems. *IEEE/ASME Transactions on Mechatronics*, 17(6):1145–1157, 2012.

[8] Samuel C Stanton, Benjamin AM Owens, and Brian P Mann. Harmonic balance analysis of the bistable piezoelectric inertial generator. *Journal of Sound and Vibration*, 331(15):3617–3627, 2012.

[9] Tian-Chen Yuan, Jian Yang, and Li-Qun Chen. A harmonic balance approach with alternating frequency/time domain progress for piezoelectric mechanical systems. *Mechanical Systems and Signal Processing*, 120:274–289, 2019.

[10] Junrui Liang and Wei-Hsin Liao. Simulation and optimization of class-e power amplifiers with extended impedance method. In *Circuits and Systems, 2009. ISCAS 2009. IEEE International Symposium on*, pages 2493–2496. IEEE, 2009.

[11] Junrui Liang and Wei-Hsin Liao. Steady-state simulation and optimization of class-e power amplifiers with extended impedance method. *IEEE Transactions on Circuits and Systems I: Regular Papers*, 58(6):1433–1445, 2011.

[12] Junrui Liang. An improvement on extended impedance method towards efficient steady-state analysis of high-frequency class-e resonant inverters. In *2018 International Power Electronics Conference (IPEC-Niigata 2018-ECCE Asia)*, pages 4122–4126. IEEE, 2018.

[13] Junrui Liang. Design of class-e power amplifier with nonlinear components by using extended impedance method. In *Circuits and Systems (ISCAS), 2016 IEEE International Symposium on*, pages 437–440. IEEE, 2016.

[14] Lihua Tang, Yue Han, James Hand, and Ryan L Harne. Exploring the roles of standard rectifying circuits on the performance of a nonlinear piezoelectric energy harvester. In *Active and Passive Smart Structures and Integrated Systems 2016*, volume 9799, page 97990J. International Society for Optics and Photonics, 2016.